CSIRO Publishing

Publications of the Astronomical Society of Australia

VOLUME 18, 2001

An international journal of astronomy and astrophysics

For editorial enquiries and manuscripts, please contact:
The Editor, PASA,
ATNF, CSIRO,
PO Box 76,
Epping, NSW 1710, Australia
Telephone: +61 2 9372 4590
Fax: +61 2 9372 4310
Email: Michelle.Storey@atnf.csiro.au

For general enquiries and subscriptions, please contact:
CSIRO Publishing
PO Box 1139 (150 Oxford St)
Collingwood, Vic. 3066, Australia
Telephone: +61 3 9662 7666
Fax: +61 3 9662 7555
Email: pasa@publish.csiro.au

Published by CSIRO Publishing
for the Astronomical Society of Australia

www.publish.csiro.au/journals/pasa

https://doi.org/10.1071/AS01033 Published online by Cambridge University Press

Publ. Astron. Soc. Aust., 2001, 18, 215–220

The Effect of Nonaxisymmetric Radiative Drag on Relativistic Jets in Active Galactic Nuclei

Qinghuan Luo

Research Centre for Theoretical Astrophysics, School of Physics,
The University of Sydney, NSW 2006, Australia

Received 2000 October 20, accepted 2001 May 23

Abstract: The effect of nonaxisymmetric radiation drag on relativistic jets in active galactic nuclei (AGN) is discussed. The radiation force due to inverse Compton scattering of photon fields from a noncircular accretion disk is calculated. It is shown that such nonaxisymmetric drag can cause jet path distortion within the subparsec region of the black hole. This subparsec scale distortion is potentially observable with the current VLBI, VLBA techniques. Any modulation of the axially asymmetric distribution of disk emission can result in variability in electromagnetic radiation from the jet.

Keywords: scattering — plasmas — relativistic jets — AGN — radiation mechanisms: nonthermal

1 Introduction

It is widely accepted that the main activities of active galactic nuclei (AGN) are powered by black holes (BHs) accreting matter through accretion disks. In such a system a relativistic jet is usually formed and accreting matter eventually releases gravitational potential energy through radiation so that the disk is a strong source of radiation fields, mainly in UV or soft X-rays. There is no single widely accepted model for the formation of an AGN jet. However, if a relativistic jet is formed sufficiently close to the putative BH, it must pass through the strong radiation field from the accretion disk and be subjected to radiative acceleration or deceleration through inverse Compton scattering. Soft photons from the disk are scattered by relativistic particles in the jet to hard X-rays or γ-rays. Such process is believed to be responsible for γ-ray emission from blazars, a class of AGN with jets directed nearly along the observer's line of sight, which have high energy γ-ray emission (von Montigny et al. 1995; Thompson et al. 1995; Gaidos et al. 1996; Quinn et al. 1996; Schubnell et al. 1996; for a theoretical model based on inverse Compton scattering see Dermer & Schlickeiser 1993).

The radiative effect on the bulk motion of relativistic jets was discussed by several authors (O'Dell 1981; Phinney 1982, 1987; Melia & Königl 1989; Sikora et al. 1996; recently Luo & Protheroe 1999, hereafter LP). O'Dell (1981), also Phinney (1982), considered radiative acceleration. The essential condition for acceleration to occur is that most of incoming photons seen in the jet frame should be directed along the jet, and this may be the case if the source is a point-like source. However, since disk emission is not point-like, this condition is generally not satisfied by a highly relativistic jet (e.g. Phinney 1982), and radiative deceleration is more relevant (Phinney 1987; Melia & Königl 1989; Sikora et al. 1996; LP).

One important assumption made in earlier discussions is that disk emission is axially symmetric. So, the only effect on the jet flow is in the jet direction (it is usually assumed that the jet is normal to the disk plane and along the spin axis of the BH). However, there are cases in which accretion may not be circular. For example, eccentric accretion can occur if the nucleus is a binary BH system with a less massive BH orbiting the more massive BH and accretion is subjected to a tidal perturbation from the secondary BH (Eracleous et al. 1995), or if there are global disk instabilities (e.g. Papaloizou & Pringle 1984, 1985; Pringle 1996, 1997), which may cause the disk to become warped or noncircular. A noncircular accretion disk gives rise to a nonaxisymmetric radiation field that depends on the azimuthal angle, and hence the radiation effect on the jet is not axisymmetric, resulting in a perpendicular (to the BH spin axis) radiation force.

The purpose of this paper is to explore Compton drag on jets by nonaxisymmetric photon fields and the resulting jet path distortion in the vicinity of the BH. Specifically, we calculate the average momentum transfer to plasmas due to inverse Compton scattering by including nonaxisymmetry in photon fields. In doing so, we assume that particles in the jet frame have an isotropic angular distribution (that is, they move in random direction). Through calculation of nonaxisymmetric drag, one may explore a possible link between subparsec jet structures to activities occurring on the disk. With the advance of VLBI and VLBA technique, subparsec structures are potentially observable (e.g. Junor & Biretta 1995), and such a link can be tested observationally. As shown in earlier work (LP) the drag effect depends on the composition of the jet, and in general, drag is reduced if jets contain a significant fraction of protons since they have a much smaller scattering cross section compared to electrons or positrons. In calculating the radiation force, scattering by protons is neglected, and protons affect the drag only by providing inertia (i.e. make jet more 'heavy').

In Section 2, a formula for calculating the radiation force in the perpendicular (to the jet flow) direction is given in the Thomson regime. A noncircular accretion

 10.1071/AS01033 1323-3580/01/03215$05.00

disk model is considered in Section 2.1, and the physical processes that produce nonaxisymmetric accretion are discussed in Section 3. Jet path distortion due to axially asymmetric drag is discussed in Section 4.

2 Compton Drag

A relativistic jet moving through an intense radiation field, e.g. radiation from an accretion disk, can be either accelerated or decelerated depending on whether particles in the jet frame see incoming photons propagating along or against the jet direction. For example, if incoming photons are in the direction against the jet flow, the jet is decelerated because more momentum is beamed (carried by scattered photons) in the jet direction through inverse Compton scattering. Radiative acceleration through inverse Compton scattering, though it can occur in principle, is ineffective because of the spatial extent of the photon distribution (Phinney 1982; Sikora et al. 1996; LP). Thus, radiative deceleration is likely to occur provided that the jet is relativistic.

To calculate radiative drag, consider a plasma cell moving with the jet and assume that there is no pair production in the cell. Although the latter assumption is not strictly accurate, it makes the calculation tractable. It is assumed that an external photon field is from an accretion disk with the photon field distribution given by $n_{\rm ph}(\varepsilon, \Omega)$, where ε is the photon energy, and $\Omega = (\phi, \cos\theta)$ is the polar angle of the photon propagation direction $\hat{\mathbf{k}}$. As plasma particles moving through the radiation field, they are slowed down because of inverse Compton scattering (Phinney 1982; 1987; Sikora et al. 1996; LP). The radiation force is thus identified as the average momentum transfer from incoming photons to the plasma. As shown in LP, an ultrarelativistic jet, even starting with a very large bulk Lorentz factor such that electrons are in the Klein-Nishina regime, is rapidly decelerated to the Thomson regime. Therefore, I only consider scattering in the Thomson limit. The radiation force ($m_e c\ {\rm s}^{-1}$ per unit volume) on the plasma cell initially moving along the z direction is given by

$$\mathbf{f} = -cn_{e0}\left\langle \int d\varepsilon \int d\Omega\, n_{\rm ph}(\varepsilon, \Omega)(1 - \beta\cos\Theta) \times \int d\varepsilon_s \int d\Omega_s \frac{d\sigma}{d\varepsilon_s d\Omega_s}\left(\varepsilon_s \hat{\mathbf{k}}_s - \varepsilon\hat{\mathbf{k}}\right)\right\rangle, \quad (1)$$

where all quantities with subscript s are for scattered photons, $d\sigma/d\varepsilon_s d\Omega_s$ is the differential cross section, βc is the electron (positron) velocity, n_{e0} is the average number density of electrons (positrons), Θ is the angle between the incoming photon and the electron motion, $\langle \ldots \rangle$ is average over the particle distribution. All quantities on the right hand side of Equation (1) are in the jet frame. In the Thomson regime, the differential cross section can be approximated by $d\sigma/d\varepsilon_s d\Omega_s \approx \sigma_{\rm T}\delta[\varepsilon_s - \gamma^2\varepsilon(1 - \beta\cos\Theta)]\delta(\Omega_s - \Omega_e)$, where $\sigma_{\rm T}$ is the Thomson cross section, $\gamma = (1 - \beta^2)^{-1/2}$, and $\Omega_e = (\phi_e, \cos\theta_e)$ is the direction of motion of the electrons (Blumenthal & Gould 1970; Reynolds 1982). The z-component of Equation (1) was calculated in detail in LP. For axisymmetric emission, $n_{\rm ph}$ and $\varepsilon\, d\varepsilon\, \sin\theta$ are independent of ϕ (in the observer's frame) and we have $f_x = f_y = 0$ and the radiation force is along the jet axis. Hence, the perpendicular components $\mathbf{f}_\perp = (f_x, f_y)$ describe nonaxisymmetric drag and are calculated in the following section.

2.1 A Nonaxisymmetric Disk Model

There is a net perpendicular force $\mathbf{f}_\perp \neq 0$ on the plasma cell when the radiation fields are not axially symmetric. A nonaxisymmetric radiation field can be due to noncircular accretion, say elliptical accretion (e.g. Eracleous et al. 1995), or due to disk warping as a result of some instability (Pringle 1996). At a radial distance sufficiently close to the BH, particle trajectories are nearly circular because of the strong gravitational field which tends to circularise the particle orbits through, for example, the Lense-Thirring effect (Thorne, Price & Macdonald 1986). In general, nonaxisymmetry can be described by an azimuthal number, m, with $m = 0$ corresponding to axisymmetry and $m = 1$ to the lowest order nonaxisymmetry (off-centre).

To calculate radiation drag, consider a noncircular disk which is planar and consists of a series of annuli with their centres being not necessarily at the same point. Assume that there are N annuli with centres at $x_1, \ldots, x_N$ on the x-axis, and the inner and outer radii are given by a_i and b_i, respectively. The coordinates are chosen such that the BH is at $x_1 = 0$. In general, such a pattern evolves as the processes that cause noncircular accretion vary on a certain time scale. Consider a plasma cell at (x, z) moving initially along the z direction. The photon energy flux density from a given ring of the ith annulus, $R \to R + \Delta R$, is axisymmetric and is represented by $F_i(\tilde{\varepsilon}, R)$ where $\tilde{\varepsilon}$ is the photon energy (in $m_e c^2$). In the following, all tilded quantities refer to the observer's frame. Then, the photon number density in the jet frame can be written as

$$n_{\rm ph}(\varepsilon, \Omega, R)dR = \frac{R\, F_i(\tilde{\varepsilon}, R)\, dR}{2\pi c\tilde{\varepsilon}} \sum_{\pm} H(|x - x_i| \pm R) \times \cos\tilde{\theta}_\pm \frac{\delta(\cos\theta - \cos\theta_\pm)}{r_\pm^2 + z^2}, \quad (2)$$

where $r_\pm = -(x - x_i)\cos\phi \pm [R^2 - (x - x_i)^2 \sin^2\phi]^{1/2}$, ϕ is the azimuthal angle with respect to the direction of motion of the cell, $\cos\tilde{\theta}_\pm = z/(r_\pm^2 + z^2)^{1/2}$, $H(x) = 1$ for $x > 0$ and $H(x) = 0$ otherwise. Note that a different definition for $F(\tilde{\varepsilon}, R)$ was used in LP where it represents the photon number flux density. Equation (2) with $\cos\tilde{\theta}_\pm$ corrects an error in Equation (2.4) in LP and also Equation (2.6) in Dermer & Schlickeiser (1993). The negative term is nonzero when x is outside the ring.

Using Equation (1) and writing $F_i(\tilde{\varepsilon}, R) = F_i(R)\delta(\tilde{\varepsilon} - \tilde{\varepsilon}_R)$ where $\tilde{\varepsilon}_R$ and $F_i(R)$ are respectively the photon energy (in $m_e c^2$) and the total flux from the ring at R, one obtains the radiation force in x-direction

$$f_x = \frac{2\sigma_{\rm T}}{3\pi} n_{e0}\Gamma\langle\gamma^2\rangle \sum_{i=1}^{N} \int_{a_i}^{b_i} dR\, R^{-1} F_i(R)\xi_i, \quad (3)$$

https://doi.org/10.1071/AS01033 Published online by Cambridge University Press

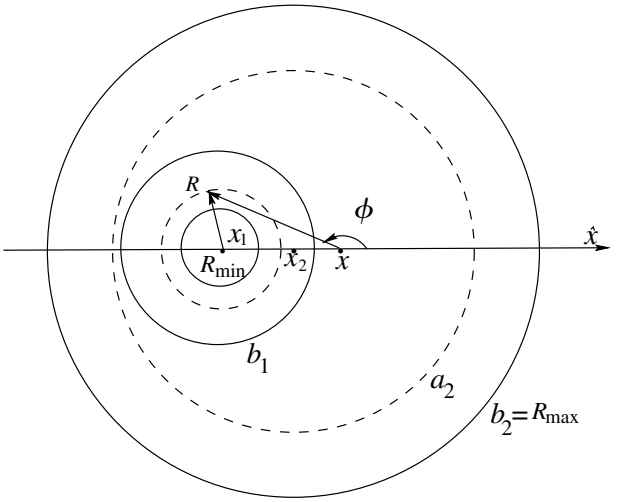

Figure 1 A model of nonaxisymmetric accretion disk consisting of two annuli with their centres shifted relative to each other (at x_1 and x_2). The BH is assumed to be at $x_1 = 0$. The inner and outer radii of the two annuli are represented respectively by a_1 ($= R_{\rm min}$) (the innermost solid circle), b_1 (the middle solid circle) and a_2 (the outer dashed circle), b_2 ($= R_{\rm max}$) (the outermost solid circle). The plasma cell is at (x, z), moving in the z-direction.

where the flux density $F_i(R)$ is in $m_e c^2\,{\rm cm}^{-2}\,{\rm s}^{-1}$, and

$$\xi_i = \sum_{\pm} \int_{\phi_0}^{\pi} d\phi\, H(|x - x_i| \pm R) \left(\frac{R}{r_\pm}\right)^2 D_\pm^{-1} \times \sin^3\tilde{\theta}_\pm \cos\tilde{\theta}_\pm \cos\phi, \tag{4}$$

with $D_\pm = 1/(1 - \beta_b \cos\tilde{\theta}_\pm)$, and $\phi_0 = \pi - \arcsin(R/|x - x_i|)$ for $|x - x_i| > R$ and $\phi_0 = 0$ otherwise. For the chosen geometry shown in Figure 1, we have $f_y = 0$. Similarly to the case of parallel drag (cf. O'Dell 1981; Phinney 1982; Sikora et al. 1996; LP), the perpendicular force is $\propto \langle\gamma^2\rangle$, and thus the relativistic effect is to enhance the drag. One noticeable difference between the parallel and perpendicular components is that f_x increases with Γ (while the parallel component, f_z, increases with Γ^2, see Equation 2.6 in LP). For $|\Delta x_i|/R \ll 1$ with $\Delta x_i = x - x_i$, the integration in Equation (4) can be carried out to obtain $\xi_i \approx (\pi/2)\,(\Delta x_i/R) G(\tilde{\theta}_R)$, where $G(\tilde{\theta}_R) = [(1 - \beta_b \cos\tilde{\theta}_R)(3 - 4\cos^2\tilde{\theta}_R) - \beta_b \cos\tilde{\theta}_R \sin^2\tilde{\theta}_R]\sin^3\tilde{\theta}_R \cos\tilde{\theta}_R$, $\tilde{\theta}_R = \tilde{\theta}_+$ with $r_+ = R$. When the disk is strictly circular, with its centre at $x = x_1 = \cdots = x_N = 0$, one has $\xi_i = 0$ at any z, corresponding to the axisymmetric drag along the jet axis.

2.2 Perpendicular Force

In general, f_x is nonzero and strongly depends on z. In the following, I consider a disk with an inner part which is circular and called the inner disk, with the centre at the BH, and an outer part, called the outer disk, which is also circular but with its centre shifted along x-axis to x_2 with respect to the inner disk. The result obtained can be extended straightforwardly to more general cases $N > 2$. To calculate (3), the corresponding inner and outer radii of the two annuli are represented by $a_1 = R_{\rm min} \le R \le b_1$ and $a_2 \le R \le b_2 = R_{\rm max}$, as shown in Figure 1. Let L_d be the disk luminosity (erg s^{-1}), and assume that most of the radiation is from the inner part of the disk. The flux density can be written as

$$F_i(R) = \frac{\chi^{i-1} L_d}{2\pi m_e c^2} F_{*i} R^{-\delta_i}, \tag{5}$$

where $i = 1, 2$ correspond respectively to the inner and outer part of the disk, F_{*i} are the normalisation constants such that radial integration gives $(1 - \chi)L_d$ (for $i = 1$) and χL_d (for $i = 2$). For a stationary accretion disk model, in which the dominant pressure is due to radiation and the dominant opacity is due to Thomson scattering, the radial scaling is typically $\delta_1 = 3$ (Shakura & Sunyaev 1973; Treves, Maraschi & Abramowicz 1988; Blandford 1990). The characteristic temperature is given by $T_s = (2\pi F/\sigma_s)^{1/4}$, where $F = m_e c^2 F_i(R)$ is the local flux density (erg cm^{-2} s^{-1}) and σ_s is the Stefan-Boltzmann constant. The outer disk is assumed to radiate reprocessed radiation (from the inner disk). Thus, the luminosity from the outer disk is only a small fraction, χ, of L_d. Since most of the disk luminosity comes from within a very small radius (less than $50R_g$ where $R_g = GM/c^2 = 1.48 \times 10^{13}\,{\rm cm}\,(M/10^8 M_\odot)$, M is the BH mass), it is reasonable to assume that the outer disk sees an isotropic radiation from the central region, and one may take for the radial scaling, $\delta_2 \approx 2$.

Substituting (5) for (3), the radiation force is expressed in term of an integration over R,

$$f_x \approx \frac{\sigma_{\rm T} n_{e0} L_d}{3\pi^2 m_e c^2}\,\Gamma\,\langle\gamma^2\rangle \sum_{i=1,2} \chi^{i-1} F_{*i} \int dR\, R^{-\delta_i - 1} \xi_i, \tag{6}$$

where ξ_i is given by (4), the integration intervals are ($R_{\rm min}$, b_1) for $i = 1$ and (a_2, $R_{\rm max}$) for $i = 2$. The first ($i = 1$) and second ($i = 2$) terms correspond respectively to the contribution from the inner and outer disk. Assuming that the electrons (positrons) have an isotropic angular distribution and their energy distribution is a power law, γ^{-p}, with the power index p, $\gamma_{\rm min} \le \gamma \le \gamma_{\rm max}$ and normalisation to n_{e0}, then, one obtains $\langle\gamma^2\rangle \approx (\gamma_{\rm min}^{p-1}\gamma_{\rm max}^{3-p} - \gamma_{\rm min}^2)(p-1)/(3-p) = 2\gamma_{\rm min}^2 \ln(\gamma_{\rm max}/\gamma_{\rm min})$ for $p = 3$.

The radiation force due to photons from the inner and outer part of the disk may have opposite sign and can cancel each other, giving zero net perpendicular force $f_x = 0$ at a certain distance, z. For $|\Delta x_i|/R \ll 1$, it can be shown from (4) that there is a characteristic height, z_i, below which the asymmetry is mainly due to the difference between the photon densities from the two regions with respectively $\Delta x_i > 0$ and $\Delta x_i < 0$, and the perpendicular force is towards the centre of the inner disk. At the height $z > z_i$, the asymmetry arises from sign change in $G(\tilde{\theta}_R)$ (cf. Equation 4), which tends to move the jet away from the centre.

An example is shown in Figure 2, in which f_x as well as the two components, f_{x1}, the force due to the inner disk,

https://doi.org/10.1071/AS01033 Published online by Cambridge University Press

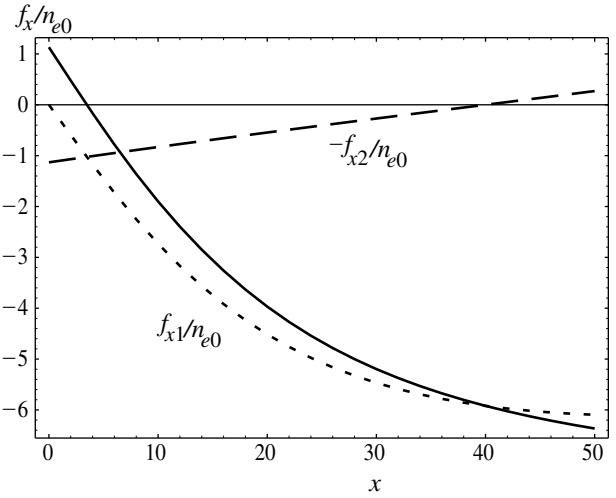

Figure 2 Plot of f_{x1}, $-f_{x2}$ and $f_x = f_{x1} + f_{x2}$ against x for $z = 50$. The disk consists of an inner part (inner disk) with radius $R_{\min} \le R \le b_1$, and an outer part (outer disk) with $a_2 \le R \le R_{\max}$. All the relevant radii, distances are in R_g. The parameters are: $L_d = 0.1 L_{\rm Edd}$, $M = 10^8\, M_\odot$, $\delta_1 = 3$, $\delta_2 = 2$, $\chi = 0.1$, $p = 3$, $\gamma_{\min} = 50$, $\gamma_{\max} = 10^4$, $\Gamma = 50$, $a_1 = R_{\min} = 6$, $b_1 = 100$, $a_2 = 200$, $b_2 = R_{\max} = 10^3$, $x_1 = 0$, $x_2 = 40$.

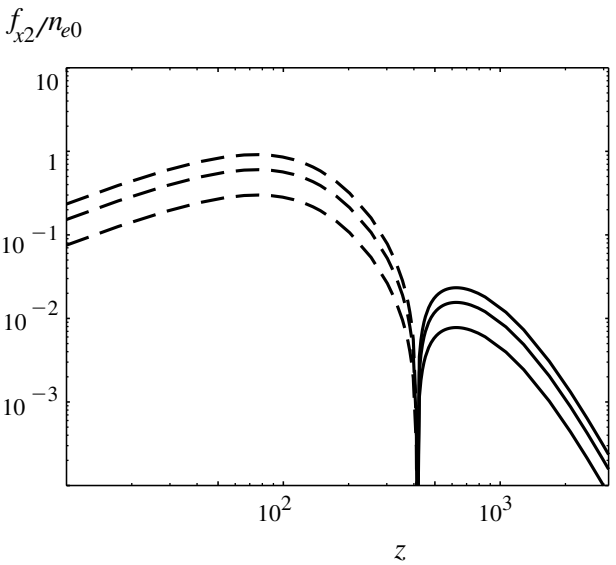

Figure 3 Plot of f_{x2} against z for $x = 10$, 20, 30 (from upper to bottom). Note that f_{x2} changes from positive sign to negative sign (with the solid curves corresponding to $f_{x2} < 0$) and $f_{x2} = 0$ at $z \approx 400$. The parameters are the same as in Figure 2, and all radii, distances are in R_g.

and f_{x2}, the force due to the outer disk, are plotted against x for $z = 50$. The plot of f_{x2} is approximately linear in x as expected from (3), and (4). The equilibrium point is at $x \approx 4$ where $f_x = f_{x1} + f_{x2} = 0$.

Figures 3 and 4 show the radiative force due to radiation from the inner and outer part of the disk. The force due to radiation from the outer disk changes sign at $z \approx 400$ from positive to negative. The location of $f_{x2} = 0$ is not very sensitive to x provided that $|\Delta x_2|/R \ll 1$. One estimates that ξ_2 changes sign when $\cos\tilde{\theta}_R > 0.68$. The

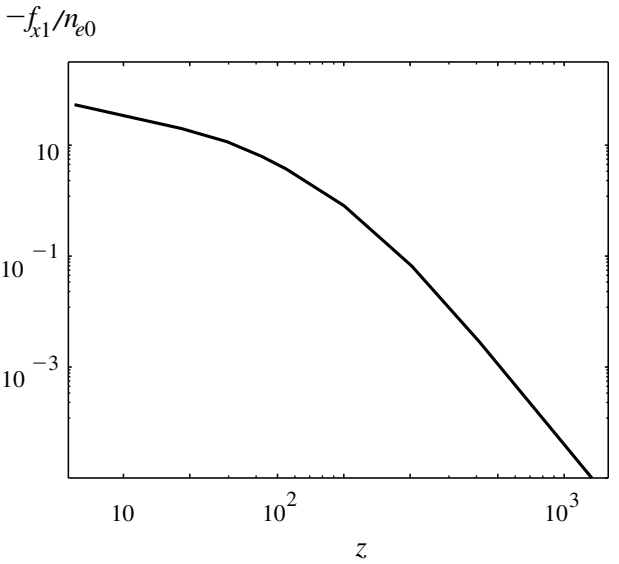

Figure 4 Plot of f_{x1} against z for $x = 20$ with the same parameters as in Figure 2.

effectiveness of drag by photons from R decreases rapidly with increasing R. Thus, f_x is important for noncircular accretion extending only to a certain radius.

3 Nonaxisymmetric Accretion

There are extensive discussions on noncircular accretion in X-ray binaries, mainly motivated by modelling the quasi-periodic variability in their light curves (e.g. Iping & Petterson 1990; Pringle 1996). However, relatively little attention has been given to noncircular accretion in AGNs. The main reason is probably that we have much more detailed observations of stellar disks compared to AGNs. As in stellar disks, axially asymmetric accretion can occur if the central object, i.e. a BH, is orbited by another less massive BH, or if a global disk instability occurs with nonaxisymmetric modes, which will be considered here in detail.

3.1 BH Binaries

Possible formation of BH binaries in AGN, as a result of mergers of galaxies, was first discussed by Begelman, Blandford & Rees (1980) and further studied in considerable detail by others, e.g. Valtaoja, Valtonen & Byrd (1989), Governato, Colpi & Maraschi (1994). During the merger, the orbital energy of the system can be efficiently removed through stellar dynamical processes, mainly the slingshot mechanism by passing stars, in a relatively short time scale $10^5 \sim 10^6$ yr. As a result, a loss-cone is formed in the stellar distribution and the stellar processes become less important in dissipating the orbital energy. During this stage, the orbital energy is removed much more slowly through stellar diffusion into the loss-cone or through a more massive BH accreting matter, and thus the binary remains stable for 10^8–10^9 yr, with a separation $a = 0.1 - 1$ pc and an orbital period given by $P_{\rm orb} \approx 280\ [q/(1+q)]^{1/2} (a/0.1\,{\rm pc})^{3/2}\ (M/10^8\,M_\odot)^{-1/2}$ yr,

https://doi.org/10.1071/AS01033 Published online by Cambridge University Press

where $q = M/m$ is the mass ratio of primary to secondary, and a is the binary separation.

Similarly to stellar disks, the disk is unstable due to tidal perturbation by the secondary, and an eccentricity develops (Lubow 1991). Using an argument analogous to stellar disk theory (e.g. Lubow 1991), one can estimate the minimum radius at which eccentricity may develop. The growth time is given by $\tau_{\rm ecc} \approx q^2 P_{\rm orb}$. For a primary with $M = 10^8\, M_\odot$, and a separation $a = 0.1$ pc, we have the orbital period $P \approx 280$ yr. The growth time for the eccentricity, e, is $\tau_{\rm ecc} \approx (M/m)^2 P = 2.8 \times 10^4$ yr for $M/m = 10$, where m is the mass of the secondary. This should be compared to the circularisation time $\tau_{\rm circ} \approx 8 \times 10^4 (M/10^8\, M_\odot)(10^5\,{\rm K}/T)^{1/2}(1+e)(R/200R_g)^2$ yr. For the eccentricity to develop, the relevant circularisation time scale must be longer than the eccentricity growth time. To make $\tau_{\rm ecc} < \tau_{\rm circ}$, one needs $R \geq 200R_g$, i.e. eccentric accretion can occur as close to the BH as $R \approx 200R_g$. When calculating f_x using the model given in Figure 1, this radius corresponds to a_2.

3.2 Disk Instability

Axial asymmetry in photon fields can arise from a global disk instability of nonaxisymmetry such as Papaloizou–Pringle instability (Papaloizou & Pringle 1984), or radiation-driven disk warping (Pringle 1996). For illustrative purposes, I only discuss the latter. Pringle (1996, 1997) has shown that disk warping may be driven by radiation from the central region of the disk. The outer part of the disk can be optically thick and irradiated by the inner part. If the outer part intercepts a sufficiently large fraction of the luminosity, the disk is unstable and becomes nonplanar. This is because the optically thick part of the disk will re-emit most of the luminosity it receives, and if irradiation is nonuniform so is re-radiation. There is a nonuniform back-reaction on the disk and thus it would induce a torque, causing the disk to warp. The minimum radius R_W, at which the warping occurs, is estimated by comparing the time scale ($\propto R^2$) for flattening locally and the time scale ($\propto R^{3/2}$) for instability to grow, that is, $R \geq R_W = 4 \times 10^3 \eta^2 (L_d/0.1 L_{\rm Edd})^{-2}$, where η is the ratio of vertical (R, z) to azimuthal (R, ϕ) viscosities (Pringle 1996). If the re-radiated luminosity is a significant fraction of L_d, the warped disk may provide a sufficient number of photons to decelerate the jet.

For a Kerr BH, disk warping may occur because of the Bardeen-Petterson effect, which is the combination of gravitomagnetic force due to BH and viscous force (Thorne et al. 1986). A disk at large radial distance, where the orientation of the disk is determined by the angular momentum of the accretion disk, is not necessarily planar and hence may not be axisymmetric. At radial distance closer to the BH, due to the Bardeen-Petterson effect, the disk orients itself to the equatorial plane of the BH so that the disk appears warped (Thorne et al. 1986). The characteristic radius for the Bardeen-Petterson effect to be important is $R \approx 10^4 R_g$.

4 Jet Path Distortion Due to Radiation Force

There is strong evidence from VLBI, VLBA observations for the existence of jets in the subparsec region such as recent VLBI images of M87 with the linear resolution of 0.01 pc (e.g. Junor & Biretta 1995) and the recent VLBA observation of NGC4151 (Ulvestad et al. 1998). An important feature of subparsec jets like M87 (also NGC4151) is the misalignment of the subparsec jet relative to the large-scale (pc or kpc) jet, suggesting that the jet is curved in the subparsec region (e.g. Zensus 1997). Such misalignment may be caused by inhomogeneous external media that confine the jet. Alternatively, it is suggested here that subparsec curvature is caused by nonaxisymmetric Compton drag provided that the subparsec jet consists mainly $e^{\pm}$. Then, one may establish a connection between the jet subparsec distortion and the disk activities such as noncircular accretion and disk instabilities.

The radiation pressure is $m_e c f_x R_j / n_{e0}$, and should be compared with the pressure of the external medium, $P_{\rm ext} = n_{\rm ext} \kappa T$, where R_j is the radius of the jet, $n_{\rm ext}$ is the number density of external plasmas, T is the temperature. Thus, the radiation pressure can be dominant when $n_{\rm ext}/n_{e0} \leq (f_x/n_{e0})\,(R_j/c)\,(m_e c^2/\kappa T) = 10^4\,(f_x/n_{e0})\,(R_j/R_g)\,(10^8\,{\rm K}/T)$. In the following, the density n_{e0} is assumed to be large so that the radiation pressure is dominant over external medium pressure (this assumption is reasonable in the region near the nucleus).

When the external medium is not important compared to radiation force, we may assume that the jet adjusts itself by shifting along x in response to the radiation pressure such that $f_x = 0$. Figure 5 shows the curves for $f_x = 0$. It is emphasised here that f_x is calculated by assuming the plasma cell is moving initially in the z direction, and hence these curves do not correspond to the exact jet trajectory. Nonetheless, since f_x strongly depends on z, the perpendicular component of the radiation force is rather inhomogeneous in the z direction, and thus, it can bend a jet. The jet emitted at $x = 0$ would bend towards the x-axis direction due to the nonaxisymmetric (with respect

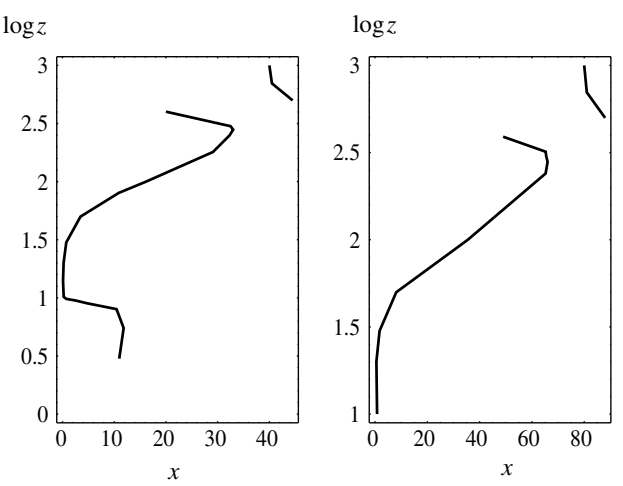

Figure 5 A trajectory for $f_x = 0$. The parameters are the same as in figure 2. Right: $x_2 = 80$.

https://doi.org/10.1071/AS01033 Published online by Cambridge University Press

to $x = 0$) radiation field from the outer part of the disk. For increasing z, the jet would curve back towards $x = 0$ axis as the force from the outer disk decreases to zero and changes sign at $z \approx 400$.

The calculation in the previous sections applies to a jet that contains protons as well. Since protons have a much smaller scattering cross section, they make negligible contribution to f_x/n_{e0} and the calculation in Section 2 is still valid. However, radiation force is reduced because protons carry a fraction of the jet luminosity, and accordingly, we have smaller $n_{e0}\bar{\gamma}$, where $\bar{\gamma}$ is the average Lorentz factor of electrons (positrons). Assume a jet starts with a luminosity $L_j = m_e c^2 n_{e0}\bar{\gamma} + m_p c^2 n_p \bar{\gamma}_p$, where $\bar{\gamma}_p$ is the average Lorentz factor of protons in the jet frame. Thus, given the same jet luminosity, compared to the pure $e^{\pm}$ jet, the radiation force would decrease by a factor of $1 + \mu_p n_p \bar{\gamma}_p/\bar{\gamma} n_{e0}$ where μ_p is the proton to electron mass ratio. It follows that the proton effect is important when $n_p/n_{e0} > \bar{\gamma}/\bar{\gamma}_p \mu_p$. For example, for cold protons with $\bar{\gamma}_p = 1$, the proton effect should be considered when $n_p/n_{e0} > 0.04$ for $\bar{\gamma} = 50$. This threshold is further reduced for relativistic protons, i.e. $\bar{\gamma}_p \gg 1$.

When radiation pressure can dominate over external medium pressure near the nucleus, nonaxisymmetric drag is the main cause for the jet distortion. Thus, the main composition of a subparsec jet with strong curvature is likely to be electrons and positrons. The $e^{\pm}$ composition of subparsec jets was also conjectured in the two-fluid model by Sol, Pelletier & Asséo (1989). In their model, $e^{\pm}$ jets are dominant only in the subparsec region and radio lobes at large scale are powered by jets with a significant fraction of protons since the proton component can transport a large luminosity to a large distance further away from the nucleus.

5 Discussion and Conclusions

Nonaxisymmetric radiative drag in relativistic AGN jets is discussed by considering a planar disk with an inner, circular disk and an outer disk that is not axisymmetric relative to the inner part. The calculation can be generalised to a nonplanar disk, say warped, with a more complicated nonaxisymmetry.

Soft photon fields from the noncircular disk are not axially symmetric, and there is a net perpendicular force, causing jet distortion in the vicinity (the subparsec region) of the BH. With current VLBI and VLBA techniques, jet curvature in the subparsec scale is potentially observable.

When jets contain a significant fraction of protons, Compton drag is reduced and jet distortion as a result of the drag is also reduced. When radiation pressure dominates over the external pressure, nonaxisymmetric drag can be a major cause of subparsec jet bending. In this case, any observed strongly curved structure in subparsec regions would favor a jet composed mainly of electrons and positrons.

Several processes that can produce axially asymmetric accretion are considered. These include eccentric accretion due to tidal perturbation by the secondary BH in a black binary, radiation induced noncircular accretion as proposed by Pringle (1996), and the Bardeen-Petterson effect. It is shown that the first two processes can cause noncircular accretion that can produce nonaxisymmetric drag. The disk warping due to the Bardeen-Petterson effect may also be important for radiation drag provided that the outer disk extends to $\sim 10^4\, R_g$.

There should be variability in electromagnetic radiation from the jet as asymmetric distribution of disk emission is temporally modulated. For a BH binary with typical parameters, the time scale is about $\geq P_{\rm orb} \approx 280$ yr, too long for the variability to be easily observable directly. However, variability due to the line-of-sight geometrical effects with a curved or helical jet might be observable.

Acknowledgements

QL thanks Ray Protheroe, Anita Mücke, and Peter Biermann for useful discussions, and the referee John Kirk for helpful comments.

References

Begelman, M. C., Blandford, R. D., & Rees, M. J. 1980, Nature, 287, 307
Blandford, R. D. 1990, in Active Galactic Nuclei, eds. R. D. Blandford, H. Netzer, & L. Woltjer (Berlin: Springer-Verlag), 161
Blumenthal, G. R., & Gould, R. J. 1970, Rev. Mod. Phys., 42, 237
Dermer, C. D., & Schlickeiser, R. 1993, ApJ, 416, 458
Eracleous, M., Livio, M., Halpern, J. P., & Storchi-Bergmann, T. 1995, ApJ, 438, 610
Gaidos, J. A., et al. 1996, Nature, 383, 319
Governato, F., Colpi, M., & Maraschi, L. 1994, MNRAS, 271, 317
Iping, R. C., & Petterson, J. A. 1990, A&A, 239, 221
Junor, W., & Biretta, J. A. 1995, AJ, 109, 500
Lubow, S. 1991, ApJ, 381, 259
Luo, Q., & Protheroe, R. J. 1999, MNRAS, 304, 800 (LP)
Melia, F., & Königl, A. 1989, ApJ, 340, 162
O'Dell, S. L. 1981, ApJ, 243, L147
Papaloizou, J. C. B., & Pringle, J. E. 1984, MNRAS, 208, 213
Papaloizou, J. C. B., & Pringle, J. E. 1985, MNRAS, 213, 799
Phinney, E. S. 1982, MNRAS, 198, 1109
Phinney, E. S. 1987, in Superluminal Radio Sources, eds. Zensus, J. A., & Pearson, T. J. (Cambridge University Press), 301
Pringle, J. E. 1996, MNRAS, 281, 357
Pringle, J. E. 1997, MNRAS, 291, 136
Quinn, J., et al. 1996, ApJ, 456, L83
Reynolds, S. P. 1982, ApJ, 256, 38
Schubnell, M. S., et al. 1996, ApJ, 460, 644
Shakura, N. I., & Sunyaev, R. A. 1973, A&A, 24, 337
Sikora, M., Sol, H., Begelman, M. C., & Madejski, G. M. 1996, MNRAS, 280, 781
Sol, H., Pelletier, G., & Asséo, E. 1989, MNRAS, 237, 411
Thompson, D. J., et al. 1995, ApJS, 101, 259
Thorne, K. S., Price, R. H., & Macdonald, D. A. 1986, Black Holes: The Membrane Paradigm (New Haven: Yale University Press)
Treves, A., Maraschi, L., & Abramowicz, M. 1988, PASP, 100, 427
Ulvestad, J. S., Roy, A. L., Colbert, E. J. M., & Wilson, A. S. 1998, ApJ, 496, 196
Valtaoja, L., Valtonen, M. J., & Byrd, G. G. 1989, ApJ, 343, 47
von Montigny, C., et al. 1995, ApJ, 440, 525
Zensus, J. A. 1997, ARA&A, 35, 607